Atmospheric Research 262 (2021) 105773

Contents lists available at ScienceDirect

Atmospheric Research

journal homepage: www.elsevier.com/locate/atmosres

Composition and sources of brown carbon aerosols in megacity Beijing during the winter of 2016

Xingru Li [a], Qing Zhao [b], Yang Yang [a], Zhengyu Zhao [a], Zirui Liu [c], Tianxue Wen [c], Bo Hu [c], Yuesi Wang [c], Lili Wang [c,*], Gehui Wang [d,*]

[a] Department of Chemistry, Capital Normal University, Beijing 100048, China
[b] College of Resource Environment and Tourism, Capital Normal University, Beijing 100048, China
[c] State Key Laboratory of Atmospheric Boundary Layer Physics and Atmospheric Chemistry, Institute of Atmospheric Physics, Chinese Academy of Sciences, Beijing 100029, China
[d] Key Laboratory of Geographic Information Science of the Ministry of Education, School of Geographic Sciences, East China Normal University, Shanghai 200241, China

ARTICLE INFO

Keywords:
Brown carbon
Chromophores
Regional transport
Source apportionments
Aqueous-phase reaction

ABSTRACT

Brown carbon (BrC) is a class of atmospheric particles that can strongly absorb visible and near-ultraviolet radiation, and it has an impact on global climate change. BrC is still poorly understood because of its complex sources and compositions. In this research, the characteristics of the light absorption, chromophores and sources of BrC were explored from $PM_{2.5}$ collected in urban Beijing during the winter of 2016. Fairly high levels of the light absorption coefficient (Abs_{λ}) of methanol-extracted BrC and two categories of chromophores, i.e., nitro-aromatic compounds (NACs) and polycyclic aromatic hydrocarbons (PAHs), were found during haze episodes, with averages of 112.4 ± 8.31 M m^{-1} (λ=365 nm), 513 ± 370 ng m^{-3} and 429 ± 244 ng m^{-3}, respectively, which were approximately 5 times higher than those during clean periods. Both methanol-extracted BrC and chromophores showed distinct diurnal variations that were twice as high during the nighttime than during the daytime. The average contributions of NACs and PAHs to the methanol-extracted BrC bulk light absorption at λ = 365 nm (Abs_{365}) were 2.30% and 1.43%, respectively, which were approximately 4.6 and 3.9 times higher than the corresponding total organic mass fractions, respectively. Correlation analyses conducted on the NACs, Abs_{365}, NO_2 and relative humidity (RH) for the clean and haze episodes indicated that the aqueous-phase reaction with higher RH had a significant impact on the BrC during haze episodes in Beijing. The source apportionment of BrC by positive matrix factorization (PMF) indicated that coal combustion (39%), secondary formation (24%), and biomass burning (28%) were the major sources of BrC in the winter in Beijing. The contribution of secondary BrC sharply increased from 16% during clan periods to 29% during haze periods, indicating that secondary formation was an important source of BrC during haze episodes. The present research provides evidence that aqueous-phase transformation has a significant impact on BrC aerosols during haze periods in urban Beijing during the winter.

1. Introduction

BrC has a significant influence on air quality, atmospheric visibility, and even climate change through its strong absorption of solar radiation in the ultraviolet and visible spectra (Park et al., 2010). Studies have reported that BrC is responsible for approximately 40% of UV–Vis absorption (Yan et al., 2018b). The direct radiative forcing (DRF) due to BrC is in the range of 0.1–0.25 Wm^{-2}, thus accounting for 10% - 25% of the DRF by black carbon (Feng et al., 2013; Liu et al., 2013; Yang et al., 2009). The light absorption of BrC is relevant not only for its morphology in the atmosphere, such as its mixing state with black carbon (BC) (Lack et al., 2012), but also for its chemical compositions and source. NACs and PAHs are ubiquitous light-absorption matter in the atmosphere (Li et al., 2019b; Lin et al., 2016; Wang et al., 2015a). NACs have an additional nitro group attached to a single aromatic ring, while PAHs have a large conjugated polycyclic structure that leads these compounds to have strong light-absorption abilities at wavelengths of 300–500 nm (Desyaterik et al., 2013; Yan et al., 2018a). Many anthropogenic activities can directly emit NACs and PAHs, including combustion of fossil fuels, biofuels, and residential coal combustion (Li et al.,

* Corresponding authors.
E-mail addresses: wll@dq.cern.ac.cn (L. Wang), ghwang@geo.ecnu.edu.cn (G. Wang).

https://doi.org/10.1016/j.atmosres.2021.105773
Received 17 February 2021; Received in revised form 6 July 2021; Accepted 17 July 2021
Available online 24 July 2021

2019a; Sumlin et al., 2017; Sun et al., 2017; Tian et al., 2019; Wong et al., 2019). Moreover, heterogeneous reactions of some volatile organic compounds (VOCs) can form secondary NACs in the presence of reactive nitrogen, such as nitrate radicals (Joo et al., 2019; Li et al., 2020a; Lin et al., 2015). Finewax et al. (2018) found that catechol can react with OH• radicals in the presence of NO_x to form 4-nitrocatechol. Other studies have shown that several NACs, such as 4-nitrophenol (4NP), 4-nitrocatechols (4NC), and methylnitrocatechols (MNCs), can be formed via aqueous reactions in the atmosphere (Kroflič et al., 2015; Pang et al., 2019; Vidović et al., 2020). The above research results indicate that complex chemical compositions and diverse sources and formation mechanisms have led to the inadequate characterization of BrC.

In recent years, biomass burning (BB), including wildfires, burning wood, and crop residue, has been used for domestic cooking and heating in winter in the rural area of the NCP (Li et al., 2010; Wang et al., 2020; Yang et al., 2020). Levoglucosan, as well as polycyclic aromatic hydrocarbons (PAHs), aromatic acids, and phenolic compounds, are abundant in the BB plum (Chakrabarty et al., 2016; Sengupta et al., 2020; Simoneit, 2002; Yunker et al., 2002). These pollutants can transport and combine with high urban/industrial emissions such as NO_x and SO_2 and then convert into low-volatility compounds to produce intensive haze pollution (Wang et al., 2015b). Cheng et al. (2013) found that approximately 50% of the OC and EC in Beijing were associated with biomass burning processes. Yan et al. (2015) found that biomass burning contributed to 17 ± 4% of the total WSOC light absorption in Beijing during winter. The contribution of biomass burning to MSOC-Abs_{365} was up to 36% in the winter of Xi'an (Yuan et al., 2020). The above studies indicated that biomass burning has a comparable contribution to particle-associated BrC.

With increasing industrialization and urbanization, the consumption of energy resources dramatically increased, and Beijing has suffered from severe particulate pollution in recent decades, especially during the winter. Previous studies on BrC in Beijing indicated that the higher MAE of WSOC in Beijing than in the southeastern United States might be due to the stronger emissions of biomass burning in China (Cheng et al., 2011). NACs contributed approximately 17% of the total absorption by methanol-extracted BrC at 370 nm in Beijing, and secondary formation and biomass burning emissions are important sources for NACs during pollution episodes (Li et al., 2020b). These studies indicated that BrC plays an essential role in heavy air pollution in Beijing. In this study, the light absorption of methanol-extracted BrC, chromophores (9 NACs and 12 PAHs), and other nonlight-absorbing organic markers was comprehensively investigated (1) diurnal variation and discrepancy in the light absorption properties, chromophore compositions of BrC and their relationships, (2) sources of BrC based on the PMF model with multiple BrC chromophores, biomass burning tracers, and water-soluble inorganic ions as inputs, and (3) different transformation pathways during haze and clean periods.

2. Experimental details

2.1. Sample collection

$PM_{2.5}$ samples were continuously collected in Beijing (BJ), an urban site in the NCP, China, for approximately two months in the winter of 2016, from November 8, 2016, to January 19, 2017. A median volume sampler (TH-150C; Wuhan Tianhong Corporation, China) with a flow rate of 100 L min^{-1} was used for $PM_{2.5}$ sampling. The samples were collected from 08:00 to 19:30 and from 20:00 to 07:30 the next day. Field blank filters were obtained as normal samples but with a 5 min pump-off period. The quartz fiber filters (Φ = 90 mm, Pall Life Sciences, USA) were prebaked at 450 °C for 4 h to eliminate the organic matter in the filter. After sampling, the filters were stored at −20 °C until analysis.

2.2. Chemical analysis

Detailed extraction, derivatization, and GC–MS analysis methods were described elsewhere (Li et al., 2019b; Li et al., 2019c). Specifically, one-quarter of each sample was cut and put into a conical flask, spiked with isotopically labeled compounds (i.e., *D*-anthracene, *D*-benzo[*a*]pyrene, C^{13}-levoglucosan, and 2,4,6-trinitrophenol) as recovery indicators, and then ultrasonically extracted three times with a dichloromethane (HPLC grade) and methanol (HPLC grade) mixture (1:2, *v*/v). Then, the combined extraction was filtered and concentrated to dryness and reacted with a mixture of 50 μL *N,O*-bis(trimethylsilyl)trifluoroacetamide (BSTFA) with 1% trimethylchlorosilane (TMCS) and 10 μL pyridine at 70 °C for 3 h. Hexamethylbenzene as the internal standard substance was added to the derivatives, and the sample was analyzed by a GC–MS system (TQ8040, Shimadzu, Japan).

An HP-5MS capillary column (30 m length, 0.25 mm diameter, 0.25 μm film thickness) was used, and high-purity helium was used as the carrier gas with a velocity of 1.0 mL min^{-1}. One microliter of the final sample solution was injected into the GC in splitless mode. The GC temperature was initially held at 50 °C for 2 min, then increased to 120 °C at 15 °C min^{-1}, isothermally held for 5 min, then increased to 290 °C at 5 °C min^{-1}, and held for 10 min at the final temperature (290 °C).

The MS was operated in electron impact (EI) mode at 70 eV, with the full scan ranging from 50 to 550 amu. The mass spectra of the target compounds were compared with standards from the National Institute of Standards and Technology (NIST) 2014. In addition, the GC–MS response factors were estimated using authentic standards. Determinations were performed by *m/z* mass chromatography, and the internal standard method was used in the quantification. All analytical procedures were controlled using strict quality assurance and control measures. Lab, field, and solvent blanks were used to determine the potential contamination. The purities of dichloromethane and methanol exceeded 99.8%. The average recoveries of the target compounds ranged from 72% to 125%. The limits of detection (LODs) were calculated using a signal-to-noise ratio of 3. LOD values were 0.30 ng μL^{-1}, 0.19–0.64 ng μL^{-1}, and 0.008–0.037 ng μL^{-1} for levoglucosan, PAHs, and nitroaromatic compounds (NACs), respectively.

Organic carbon (OC) and elemental carbon (EC) were analyzed with a DRI Model 2001 Thermal/Optical Carbon Analyzer. Details of the procedure were provided in another study (Li et al., 2019b). The inorganic ions in $PM_{2.5}$, including 4 cations (NH_4^+, K^+, Mg^{2+}, and Ca^{2+}) and 3 anions (Cl^-, NO_3^- and SO_4^{2-}), were analyzed using ion chromatography (Li et al., 2017). Detailed analysis procedures for these compositions are provided in the Supporting Materials.

2.3. Light absorption analysis

An eighth of each filter sample was extracted ultrasonically with 5 mL methanol for 20 min, and then the extraction was filtered and analyzed with a UV–Vis spectrometer (300–700 nm) (UV-2550, Shimadzu). The light absorption coefficient (Abs, Mm^{-1}) was calculated by the absorption data of all the filter extracts following eq. 1 (Xie et al., 2017):

$$Abs_\lambda = (A_\lambda - A_{700})\frac{V_l}{V_a \times L}ln(10) \quad (1)$$

where V_l (m^3) represents the volume of methanol (5 mL) used for extraction, Va (m^3) is the volume of the sampled air, L (m) is the optical path length of the quartz cuvette (1 cm) in the UV–Vis, and A_λ is the absorbance recorded from the UV–visible spectrophotometer.

The mass absorption efficiency (MAE, $m^2\ g^{-1}$) of the filter extract at a wavelength of λ is calculated using eq. 2(Bond and Bergstrom, 2006):

$$MAE_\lambda = Abs_\lambda / M \quad (2)$$

where M (gC m^{-3}) is the concentration of organic carbon in the extraction solution. In this study, organic carbon (OC) was used to replace MSOC because many studies have shown that most OC (~90%) can be extracted by methanol (Chen and Bond, 2010; Cheng et al., 2016).

The wavelength dependence for light absorption of BrC in the solution can be described by the absorption Ångström exponent (AAE). AAE was calculated through the linear regression of log (Abs) vs. log (λ) in the wavelength range of 300–550 nm (Du et al., 2014; Teich et al., 2017).

$$Abs_{\lambda} = K^{*}\lambda^{-\mathrm{AAE}} \tag{3}$$

2.4. Source apportionment of BrC by PMF

The USEPA PMF 5.0 model is a statistical factor analysis method based on the law of mass conservation and is widely used on source apportionment for typical pollutants in different environmental media (Jaeckels et al., 2007; Paatero and Tapper, 1993). The data, including the concentration and uncertainty values, are input into the model. Uncertainty (Unc) values can be estimated by the method detection limit (MDL). If the concentration is less than or equal to the MDL, the uncertainty (Unc) is calculated using a fixed fraction of the MDL (Polissar et al., 1998).

$$\mathrm{Unc} = \frac{5}{6} \times MDL \tag{4}$$

If the concentration is greater than the MDL, the calculation is based on a user-provided fraction of the concentration and MDL (eq. 5).

$$\mathrm{Unc} = \sqrt{(error\ Fraction\ concentration)^2 + (0.5 \times MDL)^2} \tag{5}$$

In this study, the MLD was calculated as 3 times the standard deviation of the blank filters, following Cacho et al. (2016). The error fraction is the precision (%) of each species, and it can be set to 5–20% depending on the concentration (Buzcu and Fraser, 2006). The error fraction in this study was assumed to be 10%.

3. Results and discussion

During sampling, the NCP experienced several serious air pollution episodes characterized by a long duration time and higher $PM_{2.5}$ and NO_2 levels, with averages of 119 ± 112 μg m-3 and 79.9 ± 38.0 μg m^{-3}, respectively (Fig. 1). The highest $PM_{2.5}$ and NO_2 reached 532 and 176 μg m^{-3}, respectively, and visibility deteriorated to 0.97 km, indicating that air pollution was relatively serious in urban Beijing during wintertime. Based on the levels of $PM_{2.5}$ and visibility, two typical stages are chosen, i.e., clean (Nov 19–24, Dec 12–16 , 2016 and Jan 8–15, 2017) and haze episodes (Dec 16–21, 2016 and Dec 29, 2016-Jan 6, 2017). The haze episodes were characterized by elevated $PM_{2.5}$ and chemical compounds (such as levoglucosan, NACs, and secondary inorganic ions) (see Table S1), which coincided with deteriorated visibility.

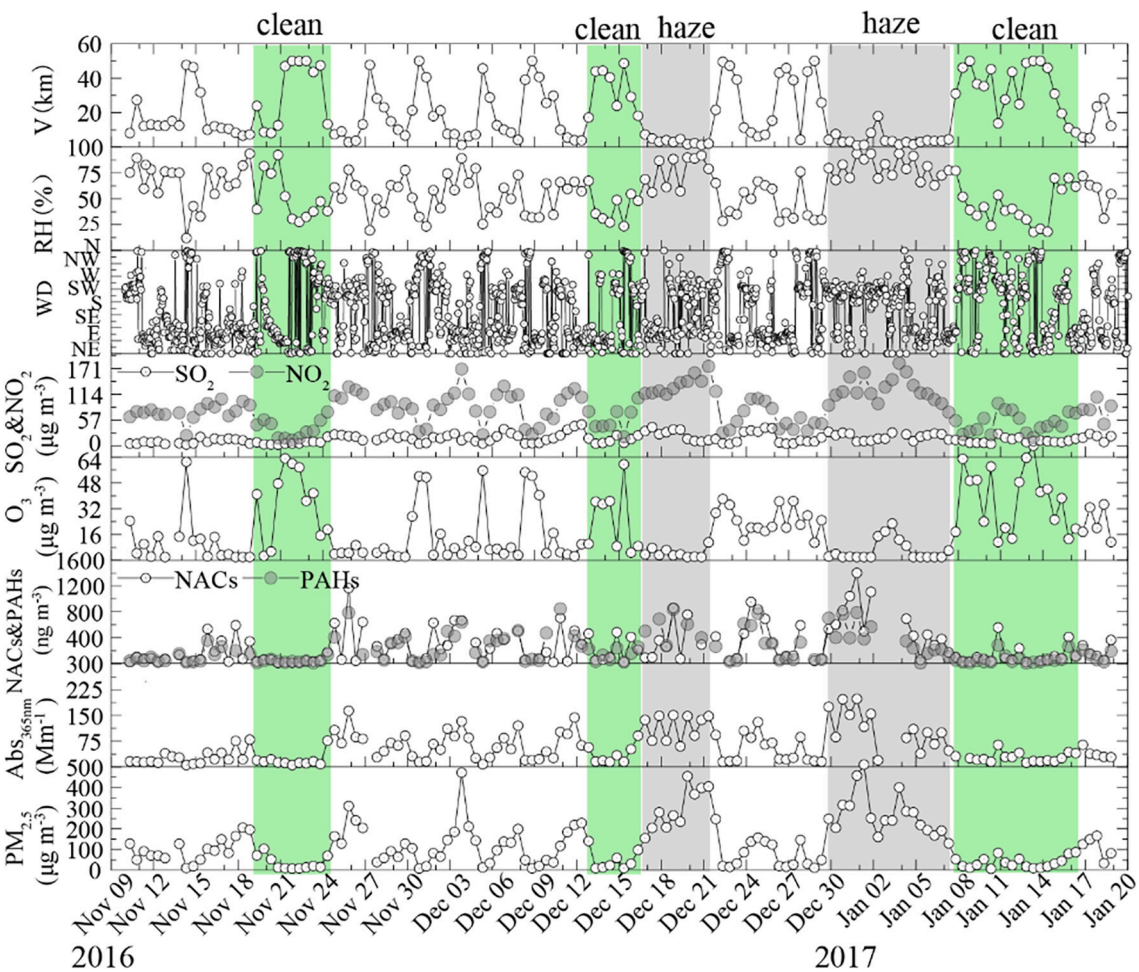

Fig. 1. Evolution of $PM_{2.5}$, Abs_{365nm}, NACs, PAHs, O_3, NO_2, SO_2, wind direction (WD), relative humidity (RH), and visibility (V) in Beijing from Nov. 8, 2016, to Jan. 19, 2017.

3.1. Abs_λ of methanol-extraction BrC

The Abs_λ values of the methanol extraction BrC were investigated at wavelengths of 300 nm, 330 nm, 365 nm, 400 nm, 450 nm, 500 nm, and 550 nm (Fig. 1). The significant feature of BrC in Beijing was that the Abs_λ decreased markedly from the ultraviolet to the visible ranges, indicating that light absorption of BrC was strongly dependent on wavelength. This trend was in accord with many other results (Cheng et al., 2016; Liu et al., 2016; Zhu et al., 2018). The average Abs_{365} of BrC was 56.9 ± 42.0 M m^{-1}, and it varied greatly between 5.19 and 197 M m^{-1}, and the highest Abs occurred at $\lambda = 300$ nm. BrC had markedly higher light absorption in the nighttime than in the daytime ($P < 0.01$) (Fig. 2 a), which was probably related to more emissions or secondary formation of absorbent substances in the nighttime and influenced by meteorological conditions. Fairly high levels of the light absorption coefficient (Abs_λ) of methanol-extracted BrC were found during haze episodes, with an average of 112.4 ± 8.31 M m^{-1} ($\lambda = 365$ nm), which were approximately 5 times higher than those during clean periods.

Compared with other studies, the average values of Abs_{365} in Beijing in this study were slightly higher than those in Xi'an (winter: 46.3 M m^{-1})(Huang et al., 2018), Indo-Gangetic Plain, India (winter: 40 ± 18 M m^{-1}) (Srinivas et al., 2016), much higher than those in Guangzhou, China (winter: 3.6 ± 1.3 M m^{-1})(Chen et al., 2018), higher than those in 2011 in Beijing (winter: 26.2 ± 18.8 M m^{-1})(Cheng et al., 2016) but lower than those in the winter of 2017 in Linfen, a typical coal-burning city in Shanxi Province, China (184 ± 46 Mm^{-1}) (Chen et al., 2019). This difference suggested the degree of air pollution to some extent. For example, the average concentrations of $PM_{2.5}$ were 75 μg m^{-3} and 119 μg m^{-3} for winter of 2011 and 2016, with the average of Abs_{365} 26.2 ± 18.8 M m^{-1} and 56.9 ± 42.0 M m^{-1}, respectively. On the other hand, this difference is also attributable to other factors such as dominance of specific sources (biomass burning, fossil fuel burning), aging processes of BrC during long range transport and meteorological conditions.

The MAE is a parameter that describes the light-absorbing ability of BrC. In this study, the MAE_{365} was slightly higher in the nighttime than in the daytime ($0.01 < P < 0.05$), with averages of 2.13 ± 0.65 m^2 g^{-1} and 1.73 ± 0.64 m^2 g^{-1}, respectively. The MAE_{365} in this study was higher than that measured in winter in other studies, such as on the Tibetan Plateau in China (Zhu et al., 2018), Xi'an in China (Huang et al., 2018), and Los Angeles in the USA (Soleimanian et al., 2020; Zhang et al., 2013) (Table S2), indicating that very strong light-absorbing chromophores existed in $PM_{2.5}$ during the winter in Beijing. Previous studies have shown that unsaturated bonds and conjugated compounds such as N-containing and S-containing compounds, HULICs and polymers which can strongly absorb the light near ultraviolet to visible spectrum (Teich et al., 2017; Zhang et al., 2013).

The AAE was calculated in the range of 300–500 nm , and the average values was 5.16 ± 1.15 and 4.07 ± 0.87 for daytime and nighttime, respectively, ranging from 3.27 to 8.39. Studies have shown that that the AAE from biomass burning and aged SOA were significantly higher compared with those from coal combustion. Significant higher AAE in the daytime than that in the nighttime ($p < 0.001$) may suggest that more BB emission or secondary BrC in the daytime, and more coal combustion in the nighttime due to indoor heating.

In general, the level of AAE values obtained here was slightly lower than that in other studies for methanol-extracted BrC, such as in Xi'an (6.0 ± 0.2)(Huang et al., 2018), Los Angeles (warm period: 7.6 ± 1.1; cold period: 8.6 ± 0.6) (Soleimanian et al., 2020), and Beijing (7.28 ± 0.24) (Cheng et al., 2016), but was comparable to that in Seoul, Korea (5.84 in winter)(Kim et al., 2016), and Delhi, India (5.1 in winter) (Kirillova et al., 2014). The value of AAE differed substantially among individual studies, ranging from 1.5 to 12(Alexander et al., 2008; Chakrabarty et al., 2010; Chen and Bond, 2010; Lewis et al., 2008). These differences were attributed not only to the compositional diversity of BrC originating from different sources but also to the aging processes of atmospheric aerosols. The slightly lower AAE values in this study than those in other urban sites in China might be related to more conjugated compounds (such as PAHs) that absorb strongly at longer wavelengths (Samburova et al., 2016).

3.2. Concentration and composition of detected BrC chromophores

Two classes of BrC chromophores were detected in this study, with 9 NACs and 12 PAHs. Diurnal variations in these organic compounds and related data in winter in Beijing are summarized in Fig. 3. The concentrations of NACs and PAHs in this study were 276 ± 293 ng m^{-3} and 213 ± 222 ng m^{-3}, respectively. Considerably higher concentrations of these compounds were found at night than during the daytime ($P < 0.001$), and they were higher during the haze period than during the clean period, which was consistent with the diurnal trends of $PM_{2.5}$ and Abs_λ. During the haze period, the average concentrations of NACs and PAHs were 513 ± 370 ng m^{-3} and 429 ± 244 ng m^{-3}, which were approximately 5.8 and 5.5 times higher than those during the clean time.

The components and mass percentages of NACs and PAHs are shown in Fig. 4. Among the detected NACs, 4NC was generally the dominant species (averaged 74.98 ± 97.95 ng m^{-3}), followed by 4NP (averaged 66.15 ± 77.40 ng m^{-3}) and 5NSA (averaged 45.67 ± 52.72 ng m^{-3}). 2,4-DNP was not detected in most samples because of the low concentration in the atmosphere, which led to an insufficient amount of data. The level

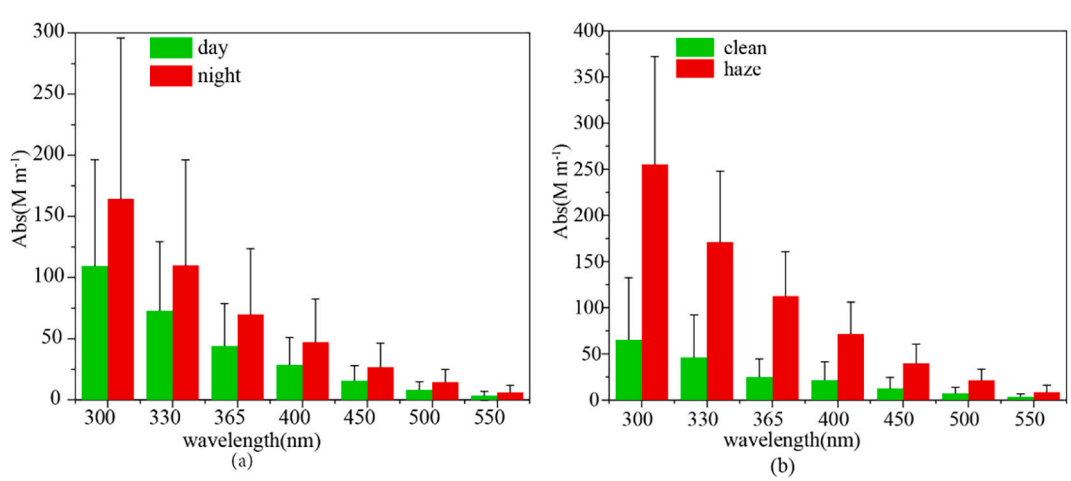

Fig. 2. Variations in the light absorption coefficients of methanol-extracted BrC. (a) Diurnal variation and (b) variations during clean and haze periods.

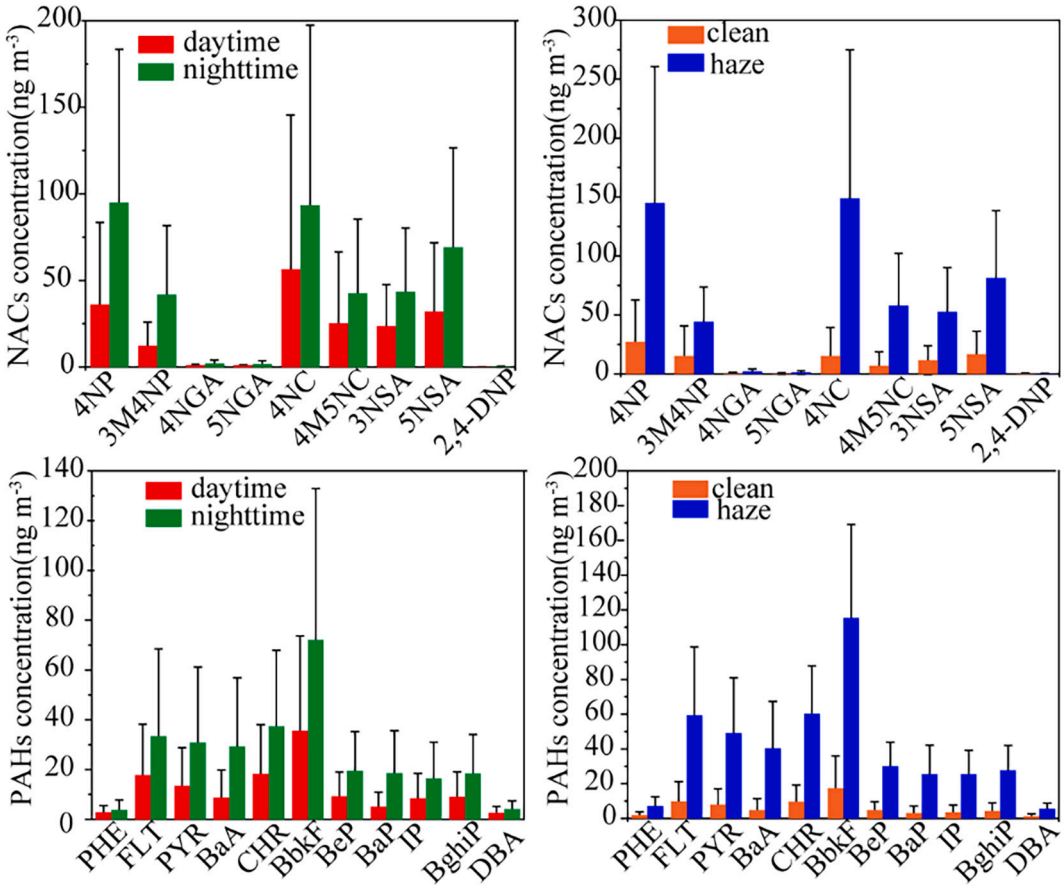

Fig. 3. Variations of NACs and PAHs.
(4NP:4-nitrophenol, 3M4NP:3-methyl-4-nitrophenol, 4NGA: 4-nitroguaiacol, 5NGA: 5-nitroguaiacol, 4NC: 4-nitrocatechol, 4M5NC:4-methyl- 5-nitrocatechol, 3NSA:3-nitrosalicylic acid, 5NSA: 5-nitrosalicylic acid, 2,4-DNP: 2,4-dinitrophenol, PHE: phenanthrene, FLU: fluoranthene, PYR: pyrene, BaA: benzanthracene, CHR: chrysene, BbkF: benzo[*b*,*k*]fluorathene, BeP: benzo[*e*]pyrene, BaP: benzo[*a*]pyrene, IP: indeno[123-*cd*]pyrene, GghiP: benzo[*ghi*]perylene, DBA: dibenzo(*a*, *h*)racanthene).

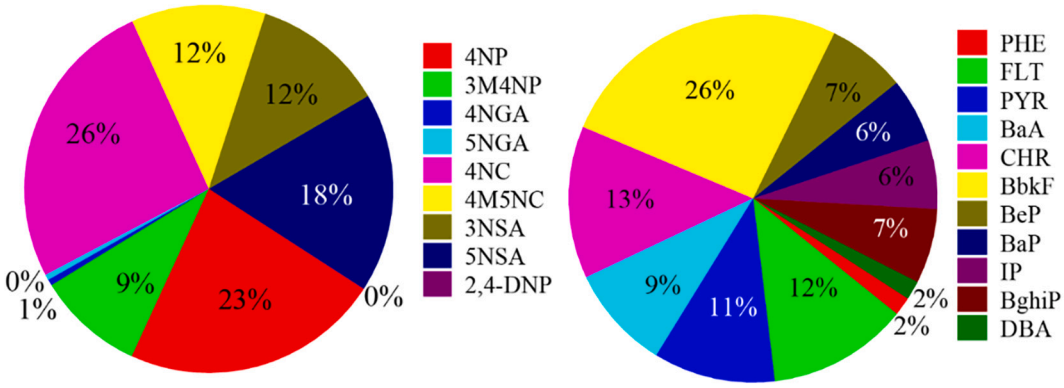

Fig. 4. Proportion of components in the detected BrC compounds.

of NACs in this study was higher than that found at other sites in winter, such as Jinan in China (48.4 ± 25.50) (Wang et al., 2018), Leipzig in Germany (14.0 ng m^{-3}) (Teich et al., 2017), Rome in Italy (39.6 ng m^{-3}) (Chow et al., 2016), and Detling in the United Kingdom (20 ng m^{-3}) (Mohr et al., 2013). Among the measured PAHs, BbkF, CHR, and FLU were the three most abundant species, contributing 27.1%, 13.9%, and 13.5% to ΣPAH mass during the daytime and 25.4%, 13.2%, and 11.8% at night, respectively. According to previous studies (Li et al., 2009; Shen et al., 2019), diagnostic ratios, such as FLU/(FLU + PYR) and BaA/(BaA + ChR), are usually used to differentiate the sources. FLU/(FLU + PYR) ratios less than 0.4, 0.4–0.5, and while values higher than 0.5 are characteristic of petroleum emission, natural gas combustion, and biomass or coal combustion (Yunker et al., 2002). A BaA/(BaA + ChR) ratio lower than 0.2 is used for petrogenic emissions, a value between 0.2 and 0.35 is used for mixtures of fossil fuel combustion, crude oil, and vehicular emissions, and a value >0.35 represents biomass and coal combustion (Yadav et al., 2018; Yunker et al., 2002). In this study, the FLU/(FLU + PYR) and BaA/(BaA + ChR) ratios during the daytime and nighttime in Beijing were mostly above 0.5 and 0.3 (Fig. S3), indicating that the combustion of biofuel and coal represented major sources of

PAHs.

To evaluate the contributions of PAHs and NACs to the light absorption of BrC, the absorption coefficients for individual BrC chromophores in this study were calculated via the following formula:

$$Abs^{*}{}_{\lambda} = MAE^{*}{}_{,\lambda} \times C_l \quad (6)$$

where $Abs^{*}{}_{\lambda}$ is the light absorption coefficient of each detected chromophore at a wavelength of λ nm, C_l is the concentration of each chromophore compound in the environment, and $MAE^{*}{}_{\lambda}$ represents the MAE of individual chromophores at a wavelength of λ nm. For a specific BrC chromophore, the $MAE^{*}{}_{\lambda}$ was obtained according to the method of Xie et al. (2017) and is listed in Table S3. The relative contributions of NACs and PAHs to the light absorption of BrC at the spectral range of 300 to 450 nm in daytime and nighttime are shown in Fig. 5.

In this study, the overall average contribution of NACs and PAHs to BrC bulk light absorption was below 10%, with a higher contribution at wavelengths shorter than 400 nm. In addition, it can be seen that the maximum value differs for individual compounds. For example, the maximum values of 4NP and 3M4NP were approximately 330 nm, the maximum wavelength of 4NC, 4 M5NC, and 4NGA was 365 nm, and the maximum wavelength of BbkF was λ = 400 nm. The mean contributions of NACs to the light absorption of BrC at λ = 365 nm were 0.14%–7.44% (averaged 1.85%) in the daytime and 0.21%–7.61% (averaged 2.70%) in the nighttime, and the contributions of PAHs were 0.04%–3.07% (averaged 1.07%) and 0.15%–5.86% (averaged 1.79%) in the daytime and nighttime, respectively. The contribution levels of NACs and PAHs to BrC bulk light absorption in this studies were about 3.7%, which was slightly higher than that observed in Xi'an in winter with the average contribution of 1.56% in winter (Yuan et al., 2020), and was the similar with the result from burning wood and charcoal in household cookstoves (1.59%–4.01%)(Xie et al., 2020), the United Kingdom (4%) (Mohr et al., 2013), and in Los Angeles, US (4%) (Zhang et al., 2013), but was lower than that reported by Li., (2020b) in Beijing (17%). The low contribution of NACs and PAHs to BrC light absorption indicates that there exists a large fraction of unknown BrC chromophores, such as HULICs and polymers. More and more evidences has shown that BrC absorption was majorly contributed by large molecules with an MW > 500–1000 Da (Di Lorenzo et al., 2017; Di Lorenzo and Young, 2016). In the future, advanced analysis techniques such as high-resolution mass spectrometry (HRMS) and nuclear magnetic resonance (NMR) should be applied to identify and characterize more BrC chromophores.

It is worth noting that this contribution was much higher than their mass contribution to the total organic mass (1.6 times OC), which was 0.50% and 0.37% for NACs and PAHs, indicating that even small amounts of these chromophores can have a disproportionately high impact on the light absorption properties of BrC.

3.3. Source apportionment of BrC using a positive matrix factorization (PMF) model

To reveal the sources and their contributions to the light absorption of BrC, the EPA PMF 5.0 model was operated. In this study, there were a total of 124 legal samples with 28 species input into the PMF 5.0 model. Fig. 6 shows the factor profiles and their contribution to Abs_{365} resolved by the model. Factor 1 was predominantly loaded with 4NP, 4NC, SO_2, PHE, FLU, and PYR. FLU, SO_2, and PYR were mainly emitted from coal combustion (Simoneit et al., 2004; Yunker et al., 2002). Moreover, 4NP has also been reported to be released from coal combustion (Lu et al., 2019; Wang et al., 2018). Therefore, factor 1 was identified as coal combustion, and it was consistent with the contribution to the Abs_{365} at 39%, and it was identified as coal combustion for heating in rural areas in the NCP in winter. The model results showed that the contribution of coal combustion to BrC was 44% and 46% under clean and haze conditions, respectively (Fig. 7), indicating that coal combustion was an important source of BrC.

Factor 2 was represented by high levels of Ca^{2+} (71%) and Mg^{2+} (84%) and a moderate loading of NO_2 (38%). Ca^{2+} and Mg^{2+} are widely considered to be from resuspended dust or soil sources. In addition, NO_2 was mainly from vehicle emissions. Therefore, this factor can be attributed to the impact of fugitive dust on vehicles. Meanwhile, the contribution of factor 2 to BrC was only 9% and reduced from 17% in the clean periods to 3% in the haze period (Fig. 7), indicating that fugitive dust contributes less to the light absorption of BrC.

The third source factor, secondary formation, was identified with the highest contributions of NH_4^+, NO_3^-, and SO_4^{2-} coupled with moderate loadings of 4NC (39%), 4M5NC (38%), NO_2 (34%), OC (34%), and EC (38%). Therefore, this factor was supposed to be related to secondary formation and vehicle emissions in the presence of NO_2 with some organic precursors or probably related to an increase in aqueous reactions ascribed to the strong hygroscopicity of secondary inorganic aerosols. The third factor contributed 24% to BrC for the whole campaign and sharply increased from 16% during clean periods to 29% during haze periods (Fig. 7), indicating that secondary formation was an important source of BrC during haze episodes. The last factor was identified as biomass burning with a contribution of 28% to the BrC for the whole campaign. This factor was more highly loaded by levoglucosan, NACs, such as 4NC, 4M5NC, 3NSA, 5NSA, and some PAH monomers, such as BaA, CHR, BbkF, and BaP. Levoglucosan is widely used as a tracer of biomass burning (Leithead et al., 2006; Simoneit et al., 1999; Zhang et al., 2008), and some 3–4 ring PAHs are considered to come from biomass burning (Jenkins et al., 1996; Rajput et al., 2011; Zheng et al., 2018). Moreover, 4NC, 4M5NC, 3NSA, and 5NSA can not only be emitted directly from biomass burning(Lin et al., 2017; Mohr et al., 2013; Wang et al., 2017) but can also be formed from volatile phenols (phenols, guaiacol, phenolic carbonyls) released from biomass

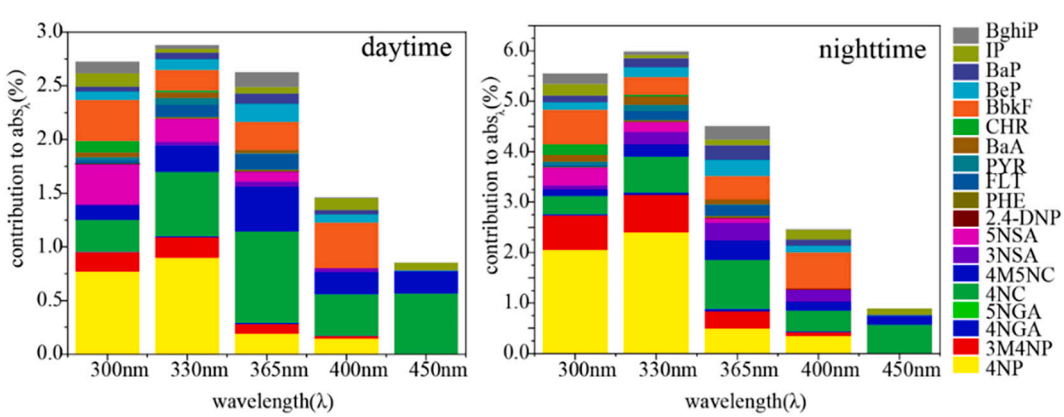

Fig. 5. Contribution of NACs and PAHs to the bulk light absorption of BrC.

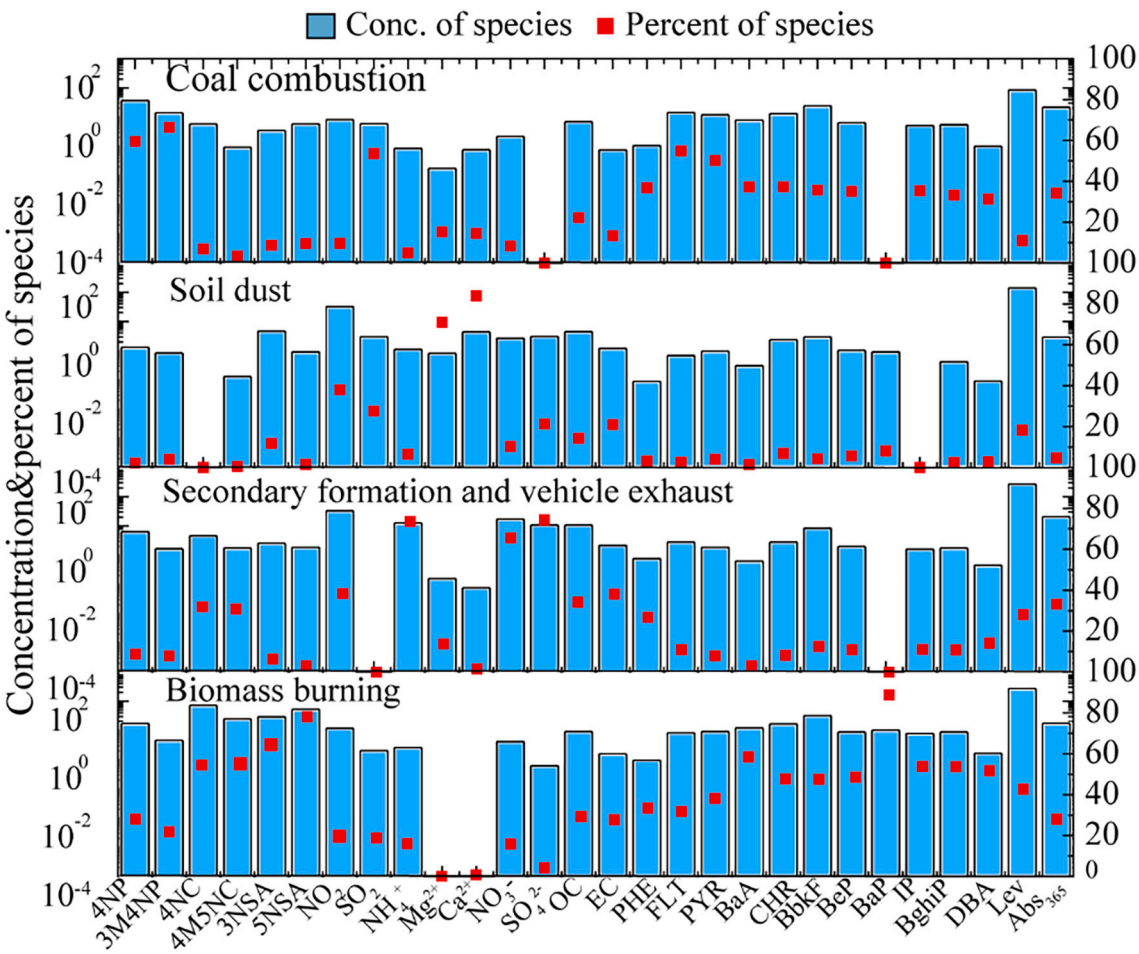

Fig. 6. Factor profiles and their contribution to Abs_{365} resolved by the model. Bars represent the concentrations of species, and the dots represent the contributions of species appointed to the factors source apportionment for airborne fine particulate BrC in Beijing during the sampling interval.

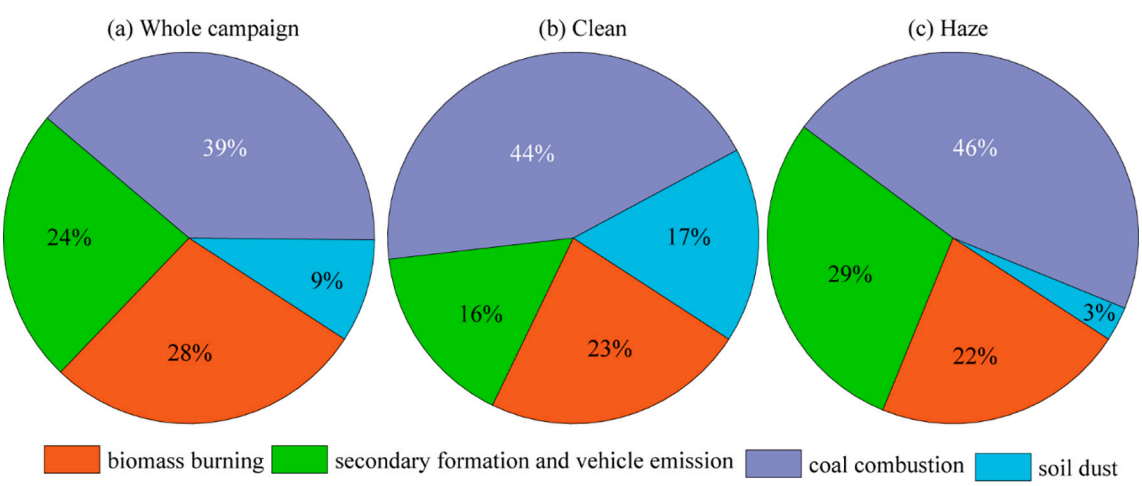

Fig. 7. Contribution of each source to the BrC loadings during the whole campaign and clean and haze periods in Beijing.

burning plumes(Chow et al., 2016; Xie et al., 2017). Therefore, this factor was considered an emission from biomass burning, with little change for clean and haze episodes.

3.4. Significant influence of aqueous transformation on BrC during the haze period

NACs are considered an important secondary BrC (Kahnt et al., 2013; Mohr et al., 2013) and can be formed via gas- and liquid-phase reactions. To better understand the formation mechanism of BrC, a series of correlation analyses were performed for the two different stages (95%

confidence interval). As shown in Fig. 8 (a) and (b), NACs and Abs_{365} were correlated well with NO_2 and poorly with RH in the clean episode, suggesting a significant impact of the gas-phase reaction with the participation of NOx in the NACs and BrCs in this stage. In contrast, marked correlations were observed between NACs and Abs_{365} and RH (Fig. 8(c)) during haze episodes, but no correlations were observed between NACs and Abs_{365} and NO_2 (Fig. 8(d)), indicating the elevated contribution of aqueous-phase pathways to NACs and secondary BrC with higher RH conditions in haze episodes. Correspondingly, the gas-phase conversion was less important for NACs and BrC. Combining the results of the PMF model, secondary formation under high RH conditions played an important role in the BrC during haze periods in urban Beijing during the winter.

Based on the above correlation results, we can suppose that during haze periods, secondary inorganic ions (NH_4^+, NO_3^- and SO_4^{2-}) were produced and accumulated to form hygroscopic particles (Wang et al., 2020). Hygroscopic particles with a high aerosol liquid water content (ALWC) can decrease the aerosol viscosity, which can increase the uptake of VOCs into the particles and the mass diffusion of reactants (Renbaum-Wolff et al., 2013; Shrestha et al., 2015; Wang et al., 2019), thus enhancing the formation of aqueous SOA. Chamber studies have also found that phenolic precursors can react rapidly in atmospheric aqueous phases to form low-volatility, light-absorbing products in the presence of reactive nitrogen species, such as NO^+, NO_2^+, NO, and NO_2(He et al., 2019; Li et al., 2020c; Pang et al., 2019; Smith et al., 2016). However, the secondary formation of NACs is still unclear and very complicated. However, it is certain that secondary formation plays an important role in the atmospheric abundance of NACs (Kahnt et al., 2013; Kitanovski et al., 2012). Their reaction mechanisms deserve further laboratory and field investigation in future studies.

4. Conclusion

In this study, the concentration levels, sources, and contributions of BrC chromophores (including 9 NACs and 12 PAHs) to the light absorption of methanol-extracted BrC were determined in winter in Beijing. Higher concentrations of NACs and PAHs were detected at a considerably higher level during haze periods. Although the contributions of NACs and PAHs to the BrC bulk light absorption were only 2.35% (ranging from 0.14%–7.61%) and 1.55% (ranging from 0.04%–5.86%), respectively, their impact on the light absorption of BrC should still not be ignored considering their very small mass proportions to the total organic mass. According to the results of the PMF model, coal combustion, secondary formation, and biomass burning were the main sources of BrC, contributing 95% to BrC. Correlation analyses indicated that aqueous-phase reactions that formed secondary BrC under higher RH conditions played an indispensable role in the notoriously bad air pollution in Beijing. The secondary formation mechanism of NACs is complex and relates not only to oxidant species and meteorological conditions but also to the physicochemical properties of $PM_{2.5}$. In the future, more attention should be focused on the identification of unknown complicated chromophores, their light absorption and the secondary formation mechanisms.

Credit authorship contribution statement

Xingru Li: Data curation, Writing – original draft; **Qing Zhao**: Writing – review & editing; **Yang Yang**: Data curation; **Zhengyu Zhao**: Methodology; **Zirui Liu**: Conceptualization; **Tianxue Wen**: Data curation; **Bo Hu**: Formal analysis; **Yuesi Wang**: Writing – review & editing; **Lili Wang**: Conceptualization, Methodology; **Gehui Wang**: Conceptualization, Methodology

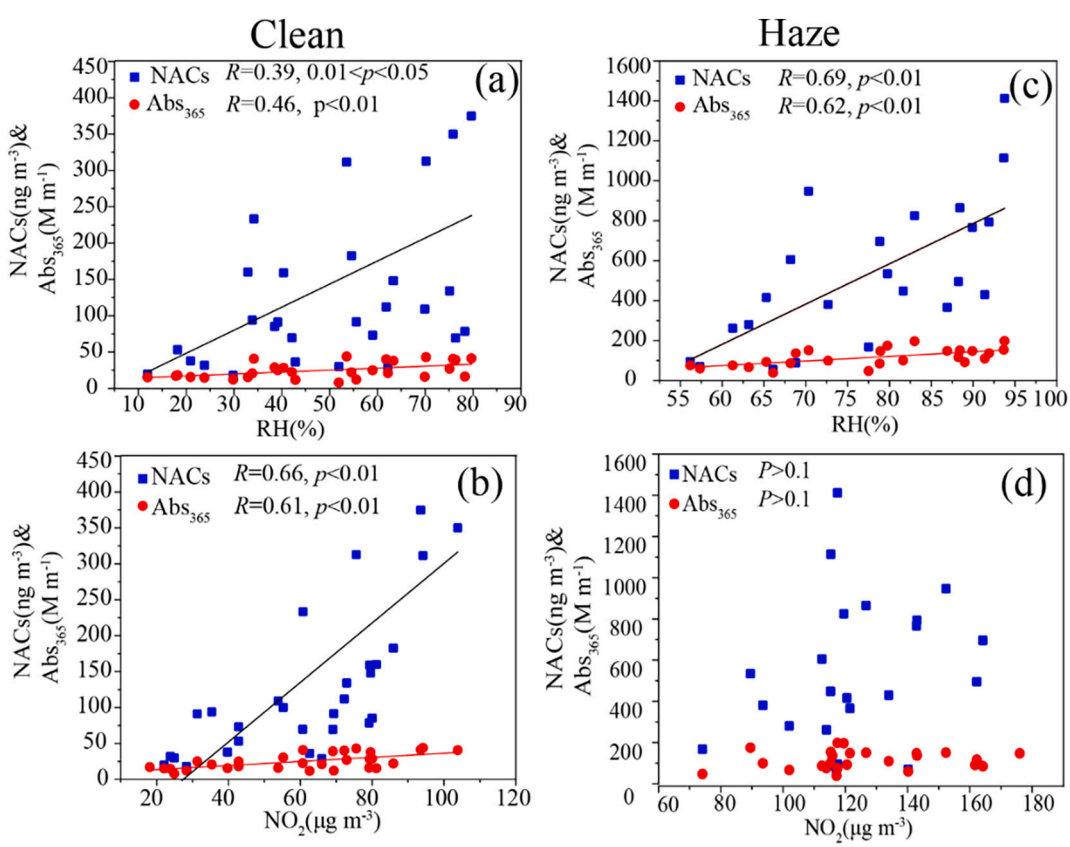

Fig. 8. Linear regression analysis for NAC and Abs_{365} with NO_2 and RH in Beijing during clean (a) and (b) haze episodes (c) and (d).

Declaration of Competing Interest

The authors declare that they have no known competing financial interests or personal relationships that could have appeared to influence the work reported in this paper.

Acknowledgments

This work was financially supported by the National Natural Science Foundation of China (NO.41905108) and the National Key R&D Program of China (No: 2017YFC0210000).

Appendix A. Supplementary data

Supplementary data to this article can be found online at https://doi.org/10.1016/j.atmosres.2021.105773.

References

Alexander, D.T.L., Crozier, P.A., Anderson, J.R., 2008. Brown carbon spheres in East Asian outflow and their optical properties. Science 321, 833–836.
Bond, T.C., Bergstrom, R.W., 2006. Light absorption by carbonaceous particles: an investigative review. Aerosol Sci. Technol. 40, 27–67.
Buzcu, B., Fraser, M.P., 2006. Source identification and apportionment of volatile organic compounds in Houston, TX. Atmos. Environ. 40, 2385–2400.
Cacho, J.I., Campillo, N., Viñas, P., Hernández-Córdoba, M., 2016. Dispersive liquid-liquid microextraction for the determination of nitrophenols in soils by microvial insert large volume injection-gas chromatography–mass spectrometry. J. Chromatogr. A 1456, 27–33.
Chakrabarty, R.K., et al., 2010. Brown carbon in tar balls from smoldering biomass combustion. Atmos. Chem. Phys. 10, 6363–6370.
Chakrabarty, R.K., et al., 2016. Brown carbon aerosols from burning of boreal peatlands: microphysical properties, emission factors, and implications for direct radiative forcing. Atmos. Chem. Phys. 16, 3033–3040.
Chen, Y., Bond, T.C., 2010. Light absorption by organic carbon from wood combustion. Atmos. Chem. Phys. 10, 1773–1787.
Chen, Y.F., et al., 2018. Seasonal light absorption properties of water-soluble brown carbon in atmospheric fine particles in Nanjing, China. Atmos. Environ. 187, 230–240.
Chen, Q.C., et al., 2019. Size-resolved characterization of the chromophores in atmospheric particulate matter from a typical coal-burning city in China. J. Geophys. Res.-Atmos. 124, 10546–10563.
Cheng, Y., et al., 2011. Mass absorption efficiency of elemental carbon and water-soluble organic carbon in Beijing, China. Atmos. Chem. Phys. 11, 11497–11510.
Cheng, Y., et al., 2013. Biomass burning contribution to Beijing aerosol. Atmos. Chem. Phys. 13, 7765–7781.
Cheng, Y., et al., 2016. The characteristics of brown carbon aerosol during winter in Beijing. Atmos. Environ. 127, 355–364.
Chow, K.S., Huang, X.H.H., Yu, J.Z., 2016. Quantification of nitroaromatic compounds in atmospheric fine particulate matter in Hong Kong over 3 years: Field measurement evidence for secondary formation derived from biomass burning emissions. Environ. Chem. 13, 665–673.
Desyaterik, Y., et al., 2013. Speciation of "brown" carbon in cloud water impacted by agricultural biomass burning in eastern China. J. Geophys. Res.-Atmos. 118, 7389–7399.
Di Lorenzo, R.A., Young, C.J., 2016. Size separation method for absorption characterization in brown carbon: Application to an aged biomass burning sample. Geophys. Res. Lett. 43, 2015GL066954 https://doi.org/10.1002/2015GL066954.
Di Lorenzo, R.A., et al., 2017. Molecular-size-separated Brown carbon absorption for biomass-burning aerosol at multiple field sites. Environ. Sci. Technol. 51, 3128–3137.
Du, Z.Y., et al., 2014. A yearlong study of water-soluble organic carbon in Beijing II: light absorption properties. Atmos. Environ. 89, 235–241.
Feng, Y., Ramanathan, V., Kotamarthi, V.R., 2013. Brown carbon: a significant atmospheric absorber of solar radiation? Atmos. Chem. Phys. 13, 8607–8621.
Finewax, Z., de Gouw, J.A., Ziemann, P.J., 2018. Identification and quantification of 4-Nitrocatechol formed from OH and NO3 radical-initiated reactions of catechol in air in the presence of NOx: implications for secondary organic aerosol formation from biomass burning. Environ. Sci. Technol. 52, 1981–1989.
He, L., Schaefer, T., Otto, T., Kroflic, A., Herrmann, H., 2019. Kinetic and theoretical study of the atmospheric aqueous-phase reactions of OH radicals with methoxyphenolic compounds. J. Phys. Chem. A 123, 7828–7838.
Huang, R.J., et al., 2018. Brown carbon aerosol in urban Xi'an, Northwest China: the composition and light absorption properties. Environ. Sci. Technol. 52, 6825–6833.
Jaeckels, J., Min-Sukbae, B., Schauer, A., 2007. Positive Matrix Factorization (PMF) analysis of molecular marker measurements to quantify the Sources of organic aerosols. Environ. Sci. Technol. 41, 5763–5769.
Jenkins, B.M., Jones, A.D., Turn, S.Q., Williams, R.B., 1996. Emission factors for polycyclic aromatic hydrocarbons from biomass burning. Environ. Sci. Technol. 30, 2462–2469.
Joo, T., Rivera-Rios, J.C., Takeuchi, M., Alvarado, M.J., Ng, N.L., 2019. Secondary organic aerosol formation from reaction of 3-methylfuran with nitrate radicals. Acs Earth Space Chem. 3, 922–934.
Kahnt, A., et al., 2013. One-year study of nitro-organic compounds and their relation to wood burning in PM10 aerosol from a rural site in Belgium. Atmos. Environ. 81, 561–568.
Kim, H., Kim, J.Y., Jin, H.C., Lee, J.Y., Lee, S.P., 2016. Seasonal variations in the light-absorbing properties of water-soluble and insoluble organic aerosols in Seoul, Korea. Atmos. Environ. 129, 234–242.
Kirillova, E.N., Andersson, A., Han, J., Lee, M., Gustafsson, Ö., 2014. Sources and light absorption of water-soluble organic carbon aerosols in the outflow from northern China. Atmos. Chem. Phys. 14, 1413–1422.
Kitanovski, Z., Grgic, I., Vermeylen, R., Claeys, M., Maenhaut, W., 2012. Liquid chromatography tandem mass spectrometry method for characterization of monoaromatic nitro-compounds in atmospheric particulate matter. J. Chromatogr. A 1268, 35–43.
Kroflič, A., Grilc, M., Grgić, I., 2015. Unraveling pathways of guaiacol nitration in Atmospheric waters: nitrite, A Source of reactive nitronium ion in the atmosphere. Environ. Sci. Technol. 49, 9150–9158.
Lack, D.A., et al., 2012. Brown carbon and internal mixing in biomass burning particles. Proc. Natl. Acad. Sci. U. S. A. 109, 14802–14807.
Leithead, A., Li, S.M., Hoff, R., Cheng, Y., Brook, J., 2006. Levoglucosan and dehydroabietic acid: evidence of biomass burning impact on aerosols in the lower fraser valley. Atmos. Environ. 40, 2721–2734.
Lewis, K., Arnott, W.P., Moosmuller, H., Wold, C.E., 2008. Strong spectral variation of biomass smoke light absorption and single scattering albedo observed with a novel dual-wavelength photoacoustic instrument. J. Geophys. Res.-Atmos. 113, 14.
Li, X.R., et al., 2009. Distribution and sources of solvent extractable organic compounds in $PM_{2.5}$ during 2007 Chinese Spring Festival in Beijing. J. Environ. Sci. 21, 142–149.
Li, W.J., Shao, L.Y., Buseck, P.R., 2010. Haze types in Beijing and the influence of agricultural biomass burning. Atmos. Chem. Phys. 10, 8119–8130.
Li, X.R., et al., 2017. Molecular composition of organic aerosol over an agricultural site in North China Plain: contribution of biogenic sources to $PM_{2.5}$. Atmos. Environ. 164, 448–457.
Li, M., et al., 2019a. Abundance and Light Absorption Properties of Brown Carbon Emitted from Residential Coal Combustion in China. Environ. Sci. Technol. 53, 595–603.
Li, X.R., et al., 2019b. Wintertime aerosol chemistry in Beijing during haze period: significant contribution from secondary formation and biomass burning emission. Atmos. Res. 218, 25–33.
Li, X.R., et al., 2019c. Spatial and seasonal variations of sugars (alcohol) in China: Emerging results from the CARE-China network. Atmos. Environ. 209, 136–143.
Li, C., et al., 2020a. Formation of secondary Brown carbon in biomass burning aerosol proxies through NO3 radical reactions. Environ. Sci. Technol. 54, 1395–1405.
Li, X., et al., 2020b. Characterizing chemical composition and light absorption of nitroaromatic compounds in the winter of Beijing. Atmos. Environ. 237, 117712.
Li, X., et al., 2020c. Light absorption properties of brown carbon (BrC) in autumn and winter in Beijing: Composition, formation and contribution of nitrated aromatic compounds. Atmos. Environ. 223, 117289.
Lin, P., et al., 2015. Molecular characterization of Brown carbon (BrC) chromophores in secondary organic aerosol generated from photo-oxidation of toluene. Phys. Chem. Chem. Phys. 17, 23312–23325.
Lin, P., et al., 2016. Molecular characterization of brown carbon in biomass burning aerosol particles. Environ. Sci. Technol. 50, 11815–11824.
Lin, P., et al., 2017. Molecular chemistry of atmospheric Brown carbon inferred from a nationwide biomass burning event. Environ. Sci. Technol. 51, 11561–11570.
Liu, J., et al., 2013. Size-resolved measurements of brown carbon in water and methanol extracts and estimates of their contribution to ambient fine-particle light absorption. Atmos. Chem. Phys. 13, 12389–12404.
Liu, J., et al., 2016. Optical properties and aging of light-absorbing secondary organic aerosol. Atmos. Chem. Phys. 16, 12815–12827.
Lu, C., et al., 2019. Emissions of fine particulate nitrated phenols from residential coal combustion in China. Atmos. Environ. 203, 10–17.
Mohr, C., et al., 2013. Contribution of nitrated phenols to wood burning brown carbon light absorption in Detling, United Kingdom during winter time. Environ. Sci. Technol. 47, 6316–6324.
Paatero, P., Tapper, U., 1993. Analysis of different modes of factor-analysis as least-squares fit problems. Chemom. Intell. Lab. Syst. 18, 183–194.
Pang, H., et al., 2019. Nitrite-mediated photooxidation of vanillin in the atmospheric aqueous phase. Environ. Sci. Technol. 53, 14253–14263.
Park, R.J., Kim, M.J., Jeong, J.I., Youn, D., Kim, S., 2010. A contribution of brown carbon aerosol to the aerosol light absorption and its radiative forcing in East Asia. Atmos. Environ. 44, 1414–1421.
Polissar, A.V., Hopke, P.K., Paatero, P., Malm, W.C., Sisler, J.F., 1998. Atmospheric aerosol over Alaska: 2. Elemental composition and sources. J. Geophys. Res. 103, 19045–19057.
Rajput, P., Sarin, M.M., Rengarajan, R., Singh, D., 2011. Atmospheric polycyclic aromatic hydrocarbons (PAHs) from post-harvest biomass burning emissions in the Indo-Gangetic Plain: Isomer ratios and temporal trends. Atmos. Environ. 45, 6732–6740.
Renbaum-Wolff, L., et al., 2013. Viscosity of α−pinene secondary organic material and implications for particle growth and reactivity. Proc. Natl. Acad. Sci. 110, 8014–8019.

Samburova, V., et al., 2016. Polycyclic aromatic hydrocarbons in biomass-burning emissions and their contribution to light absorption and aerosol toxicity. Sci. Total Environ. 568, 391–401.
Sengupta, D., et al., 2020. Polar semivolatile organic compounds in biomass-burning emissions and their chemical transformations during aging in an oxidation flow reactor. Atmos. Chem. Phys. 20, 8227–8250.
Shen, R.R., et al., 2019. Atmospheric levels, variations, sources and health risk of $PM_{2.5}$-bound polycyclic aromatic hydrocarbons during winter over the North China Plain. Sci. Total Environ. **655**, 581–590.
Shrestha, M., et al., 2015. On surface order and disorder of α-pinene-derived secondary organic material. J. Phys. Chem. A 119, 4609–4617.
Simoneit, B.R.T., 2002. Biomass burning — a review of organic tracers for smoke from incomplete combustion. Appl. Geochem. 17, 129–162.
Simoneit, B.R.T., et al., 1999. Levoglucosan, a tracer for cellulose in biomass burning and atmospheric particles. Atmos. Environ. 33, 173–182.
Simoneit, B.R.T., Kobayashi, M., Mochida, M., Kawamura, K., Huebert, B.J., 2004. Aerosol particles collected on aircraft flights over the northwestern Pacific region during the ACE-Asia campaign: Composition and major sources of the organic compounds. J. Geophys. Res.-Atmos. 109.
Smith, J.D., Kinney, H., Anastasio, C., 2016. Phenolic carbonyls undergo rapid aqueous photodegradation to form low-volatility, light-absorbing products. Atmos. Environ. 126, 36–44.
Soleimanian, E., Mousavi, A., Taghvaee, S., Shafer, M.M., Sioutas, C., 2020. Impact of secondary and primary particulate matter (PM) sources on the enhanced light absorption by brown carbon (BrC) particles in Central Los Angeles. Sci. Total Environ. 705, 135902.1–135902.11.
Srinivas, B., Rastogi, N., Sarin, M.M., Singh, A., Singh, D., 2016. Mass absorption efficiency of light absorbing organic aerosols from source region of paddy-residue burning emissions in the Indo-Gangetic Plain. Atmos. Environ. 125, 360–370.
Sumlin, B.J., et al., 2017. Atmospheric photooxidation diminishes light absorption by primary Brown carbon aerosol from biomass burning. Environ. Sci. Tech. Let. 4, 540–545.
Sun, J.Z., et al., 2017. Emission factors and light absorption properties of brown carbon from household coal combustion in China. Atmos. Chem. Phys. 17, 4769–4780.
Teich, M., et al., 2017. Contributions of nitrated aromatic compounds to the light absorption of water-soluble and particulate brown carbon in different atmospheric environments in Germany and China. Atmos. Chem. Phys. 17, 1653–1672.
Tian, J., et al., 2019. Emission characteristics of primary Brown carbon absorption from biomass and coal burning: development of an optical emission inventory for China. J. Geophys. Res.-Atmos. 124, 1879–1893.
Vidović, K., Kroflič, A., Šala, M., Grgić, I., 2020. Aqueous-phase Brown carbon formation from aromatic precursors under sunlight conditions. Atmosphere-Basel 11, 131.
Wang, J.Z., et al., 2015a. Characteristics and major sources of carbonaceous aerosols in $PM_{2.5}$ from Sanya, China. Sci. Total Environ. **530**, 110–119.
Wang, L.L., Xin, J.Y., Li, X.R., Wang, Y.S., 2015b. The variability of biomass burning and its influence on regional aerosol properties during the wheat harvest season in North China. Atmos. Res. 157, 153–163.
Wang, X., et al., 2017. Emissions of fine particulate nitrated phenols from the burning of five common types of biomass. Environ. Pollut. 230, 405–412.
Wang, L., et al., 2018. Observations of fine particulate nitrated phenols in four sites in northern China: Concentrations, source apportionment, and secondary formation. Atmos. Chem. Phys. 18, 4349–4359.
Wang, Y., et al., 2019. The formation of nitro-aromatic compounds under high NOx and anthropogenic VOC conditions in urban Beijing, China. Atmos. Chem. Phys. 19, 7649–7665.
Wang, J., et al., 2020. Enhanced aqueous-phase formation of secondary organic aerosols due to the regional biomass burning over North China Plain. Environ. Pollut. 256, 113401.
Wong, J.P.S., et al., 2019. Atmospheric evolution of molecular-weight-separated brown carbon from biomass burning. Atmos. Chem. Phys. 19, 7319–7334.
Xie, M., et al., 2017. Light absorption of secondary organic aerosol: composition and contribution of nitroaromatic compounds. Environ. Sci. Technol. 51, 11607–11616.
Xie, M., et al., 2020. Chemical composition, structures, and light absorption of N-containing aromatic compounds emitted from burning wood and charcoal in household cookstoves. Atmos. Chem. Phys. 20, 14077–14090.
Yadav, I.C., Devi, N.L., Li, J., Zhang, G., 2018. Polycyclic aromatic hydrocarbons in house dust and surface soil in major urban regions of Nepal: Implication on source apportionment and toxicological effect. Sci. Total Environ. 616-617, 223–235.
Yan, C., et al., 2015. Chemical characteristics and light-absorbing property of water-soluble organic carbon in Beijing: Biomass burning contributions. Atmos. Environ. 121, 4–12.
Yan, J., Wang, X., Gong, P., Wang, C., Cong, Z., 2018a. Review of brown carbon aerosols: recent progress and perspectives. Sci. Total Environ. 634, 1475–1485.
Yan, J.P., Wang, X.P., Gong, P., Wang, C.F., Cong, Z.Y., 2018b. Review of brown carbon aerosols: recent progress and perspectives. Sci. Total Environ. 634, 1475–1485.
Yang, M., Howell, S.G., Zhuang, J., Huebert, B.J., 2009. Attribution of aerosol light absorption to black carbon, brown carbon, and dust in China - interpretations of atmospheric measurements during EAST-AIRE. Atmos. Chem. Phys. 9, 2035–2050.
Yang, Y., et al., 2020. Seasonal variation and sources of derivatized phenols in atmospheric fine particulate matter in North China Plain. J. Environ. Sci.-China 89, 136–144.
Yuan, W., et al., 2020. Characterization of the light-absorbing properties, chromophore composition and sources of Brown carbon aerosol in Xi'an, northwestern China. Atmos. Chem. Phys. 20, 5129–5144.
Yunker, M.B., et al., 2002. PAHs in the Fraser River basin: a critical appraisal of PAH ratios as indicators of PAH source and composition. Org. Geochem. 33, 489–515.
Zhang, T., et al., 2008. Identification and estimation of the biomass burning contribution to Beijing aerosol using levoglucosan as a molecular marker. Atmos. Environ. 42, 7013–7021.
Zhang, X., Ying-Hsuan, L., Surratt, J.D., Weber, R.J., 2013. Sources, composition and absorption ?ngstr?m exponent of light-absorbing organic components in aerosol extracts from the Los Angeles Basin. Environ. Sci. Technol. 47, 3685–3693.
Zheng, H., et al., 2018. Biomass burning contributed most to the human cancer risk exposed to the soil-bound PAHs from Chengdu Economic Region, western China. Ecotoxicol. Environ. Saf. 159, 63–70.
Zhu, C.S., et al., 2018. Light absorption properties of brown carbon over the southeastern Tibetan Plateau. Sci. Total Environ. 625, 246–251.